

Supporting information

The Reaction Mechanism and Capacity Degradation Model in Lithium Insertion Organic Cathodes, $\text{Li}_2\text{C}_6\text{O}_6$, Using Combined Experimental and First Principle Studies

Haegyeom Kim,^a Dong-Hwa Seo,^a Gabin Yoon,^{a,b} William A. Goddard III,^c Yun Sung Lee,^{d} Won-Sub Yoon,^{e*} and Kisuk Kang^{a,b*}*

a. Department of Materials Science and Engineering, Research Institute of Advanced Materials (RIAM), Seoul National University, Gwanak-ro 599, Gwanak-gu, Seoul 151-742, Republic of Korea.

b. Center for nanoparticle research, Institute for Basic Science (IBS), Seoul National University, Gwanak-ro 599, Gwanak-gu, Seoul 151-742, Republic of Korea.

c. Materials and Process Simulation Center (MC 139-74), California Institute of Technology, 12000 East California Boulevard, Pasadena, CA, 91125, USA.

d. Faculty of Applied Chemical Engineering, Chonnam National University, Gwangju 500-757, Republic of Korea

e. Department of Energy Science, Sungkyunkwan University, Suwon 440-746, Republic of Korea.

Corresponding Author

Yun Sung Lee, E-mail address: leeys@chonnam.ac.kr

Won-Sub Yoon, E-mail address: wsyoon@skku.edu

Kisuk Kang, E-mail address: matlgen1@snu.ac.kr

Tel.: +82-2-880-7088 Fax.: +82-2-885-9671

Experimental

Synthesis of $\text{Li}_2\text{C}_6\text{O}_6$

The preparation of $\text{Li}_2\text{C}_6\text{O}_6$ samples was conducted as described previously.¹ Briefly, 2 g of commercial rhodizonic acid dihydrate ($\text{H}_2\text{C}_6\text{O}_6 \cdot 2\text{H}_2\text{O}$, 98%; Alfa Aesar, Ward Hill, MA, USA) and 0.713 g of lithium carbonate (Li_2CO_3 , >99%; Sigma-Aldrich, St. Louis, MO, USA) were mixed in a mortar. Deionized (DI) water (20 mL) was added slowly to the mixture and stirred for 12 h. After the solution was centrifuged for 10 min at 8000 rpm, the precipitated powder was rinsed with acetone (25 mL) and dried in a vacuum oven for 10 h. The obtained powder was heated at 200°C under an argon (Ar) atmosphere for 17 h to obtain the final product.

Sample characterization

Structural analyses of $\text{Li}_2\text{C}_6\text{O}_6 \cdot 2\text{H}_2\text{O}$ and $\text{Li}_2\text{C}_6\text{O}_6$ were performed with an X-ray diffractometer (D2PHASER; Bruker, Billerica, MA, USA) using Cu K_α radiation over a scan range of 12°–52°. The morphology of the samples was investigated using a field-emission scanning electron microscope (FE-SEM; SUPRA 55VP; Carl Zeiss, Oberkochen, Germany). Fourier transform infrared (FT-IR; Hyperion 3000; Bruker) spectra were collected from 600 to 3000 cm^{-1} . Thermogravimetry/differential scanning calorimetry (TG/DSC) experiments were performed in a nitrogen atmosphere at a heating rate of 5°C min^{-1} .

Electrochemical characterization

Electrodes were prepared by mixing the active material ($\text{Li}_2\text{C}_6\text{O}_6$, 60 wt%) with a polyvinylidene fluoride binder (10 wt%) and conductive carbon (Super-P, 30 wt%; MTI

Corporation, Richmond, CA, USA) in *N*-methyl-2-pyrrolidone. The resulting slurry was spread uniformly onto aluminum foil and dried at 30°C under vacuum for 12 h followed by roll-pressing. Test cells were assembled into a two-electrode configuration in a glove box. The cells consisted of a Li metal counter electrode, a separator (Celgard 2400; Celgard, Charlotte, NC, USA), and an electrolyte composed of 1 M lithium hexafluorophosphate in a 1:1 mixture of ethylene carbonate and dimethyl carbonate (Techno Semichem, Seongnam-Si, Gyeonggi, Korea). Cyclic voltammograms were obtained from 3.5 to 1.5 V using a multichannel potentiogalvanostat (WonATech, Seoul, Korea). Quasi-open-circuit potential (QOCP) measurements were performed using a constant current of 20 mA g⁻¹. The electrochemical cells were discharged and charged for 1 h with 2-h relaxation times. Potentiostatic intermittent titration technique (PITT) measurements were conducted using a “staircase” voltage profile in which the cell potential was changed in 5-mV increments. The current was measured at each constant potential step. Each individual titration was finished when the absolute current reached 10 mA g⁻¹.

Computational details

First principles density functional theory (DFT) calculations were performed with the spin-polarized Generalized Gradient Approximation (GGA) and the Perdew–Burke–Ernzerhof (PBE) exchange–correlation parameterization.² The Vienna *ab initio* simulation package (VASP) was employed with a plane-wave basis and the projector-augmented wave (PAW) method.³ The DFT-ulg method was used to account for van der Waals interactions between molecules. This method consists of adding a low-gradient (lg) pairwise dispersion potential to the conventional Kohn–Sham DFT Hamiltonian.⁴ Energy calculations were performed in the $1a \times 2b \times 2c$ supercell of a Li₄C₆O₆ crystal containing 8 formula units (f.u.). A plane-wave

basis with a kinetic energy cutoff of 500 eV and $2 \times 2 \times 3$ Monkhorst–Pack k -point meshes were used to ensure that the total energies converged within 5 meV per f.u.

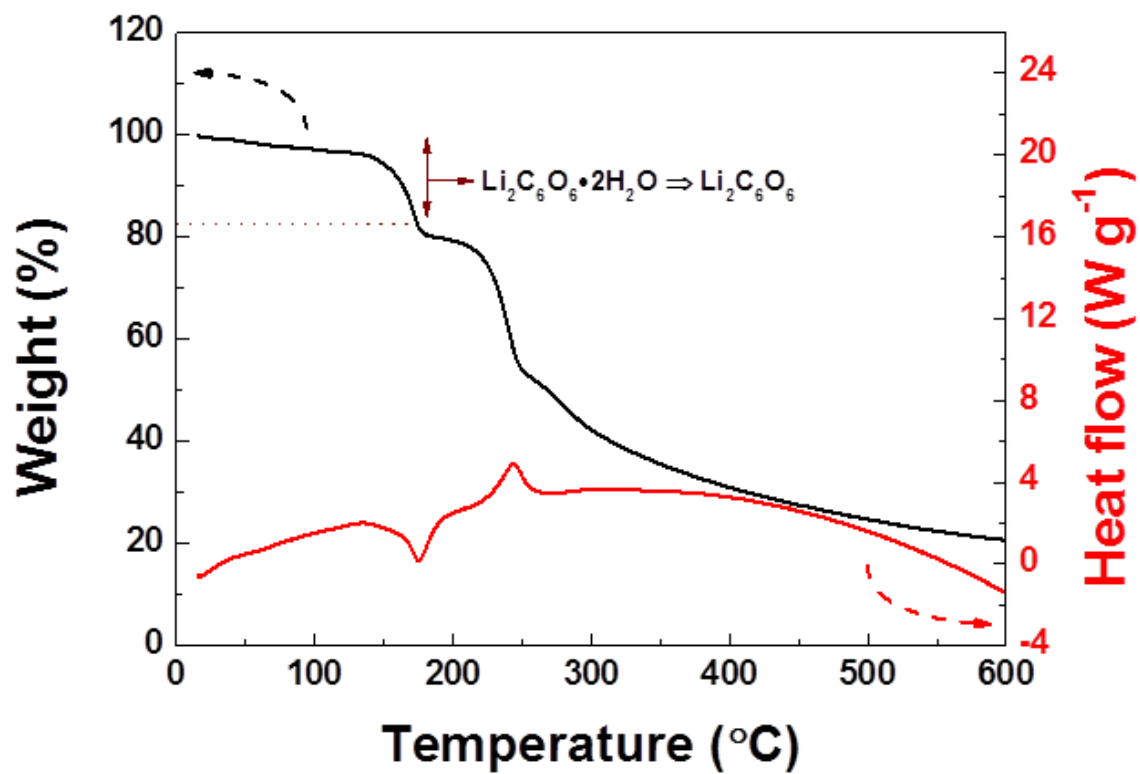


Figure S1. TGA/DSC analyses of the $\text{Li}_2\text{C}_6\text{O}_6$ electrode material from room temperature to 600 $^{\circ}\text{C}$. Water was removed from the $\text{Li}_2\text{C}_6\text{O}_6 \cdot 2\text{H}_2\text{O}$ at $\sim 180^{\circ}\text{C}$.

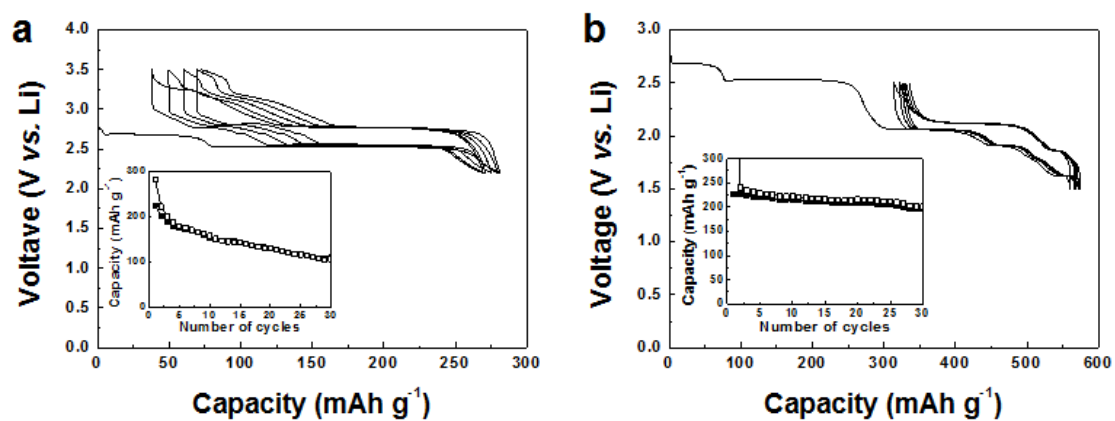


Figure S2. Charge/discharge profiles of Li₂C₆O₆ are shown from **a.** 2.2 to 3.5 V, corresponding to the electrochemical reaction from Li₂C₆O₆ to Li₄C₆O₆ (the inset shows a typical cyclability measurement) and from **b.** 1.5 to 2.5 V, corresponding to the electrochemical reaction from Li₄C₆O₆ to Li₆C₆O₆ (the inset shows a typical cyclability measurement).

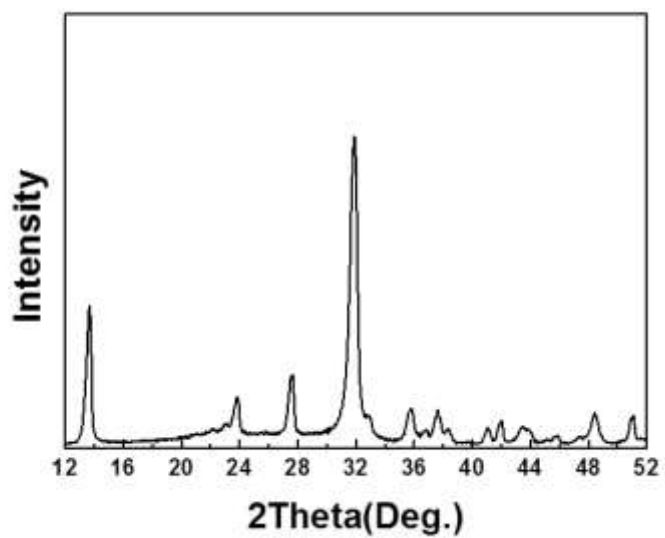


Figure S3. XRD pattern of $\text{Li}_4\text{C}_6\text{O}_6$ synthesized by heating $\text{Li}_2\text{C}_6\text{O}_6$ powder at 400°C .

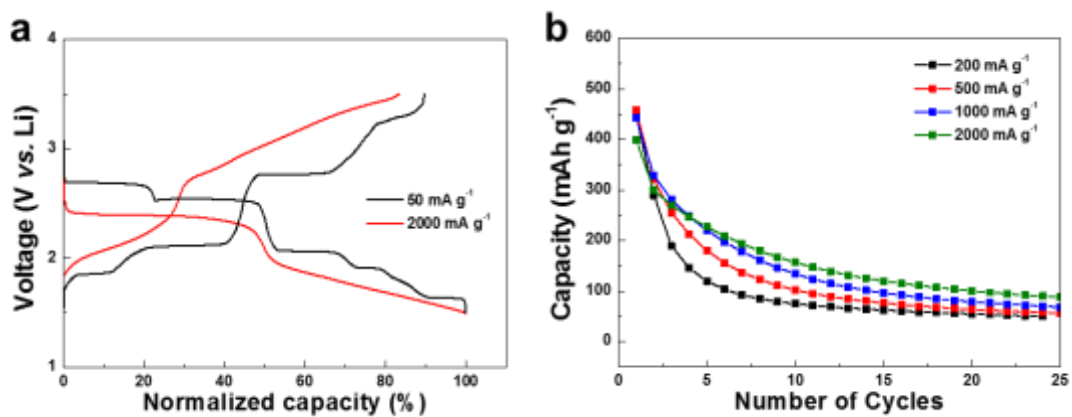


Figure S4 a. Charge/discharge profiles of $\text{Li}_2\text{C}_6\text{O}_6$ at 50 mA g^{-1} and 2000 mA g^{-1} . **b.** Cycle stability at various current rates.

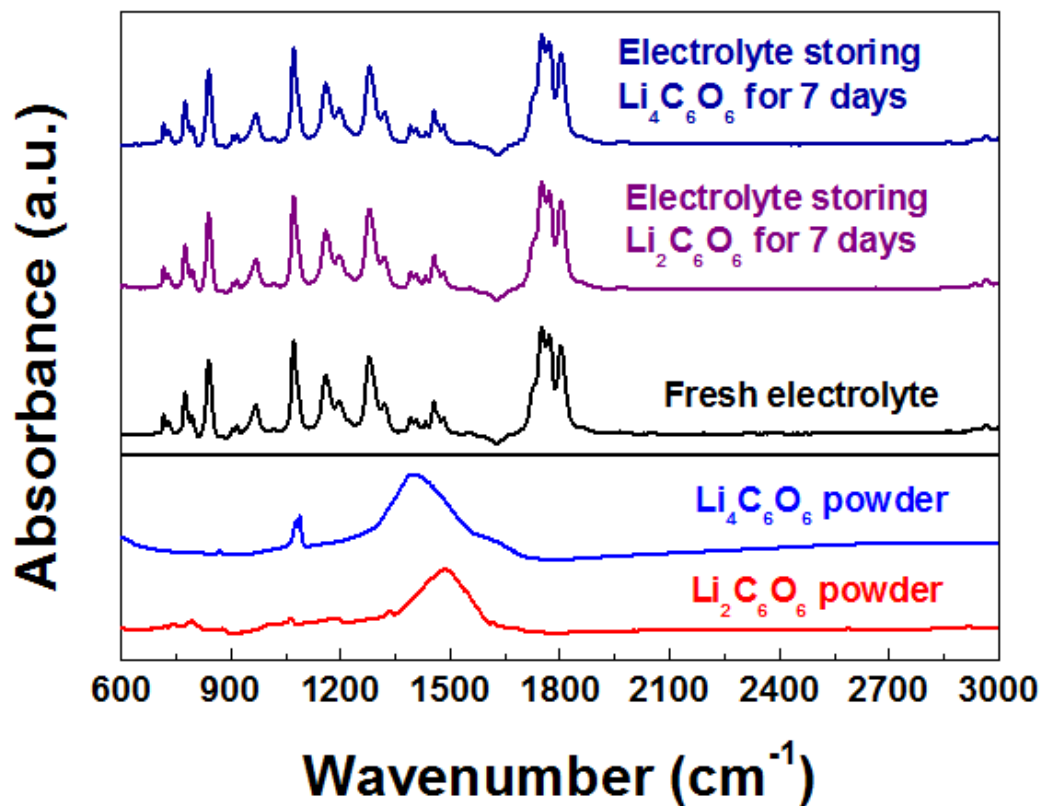


Figure S5. Fourier transform infrared (FT-IR) spectroscopic analyses were performed on electrolytes that had contained $\text{Li}_2\text{C}_6\text{O}_6$ and $\text{Li}_4\text{C}_6\text{O}_6$ for 7 days. The concentration of $\text{Li}_2\text{C}_6\text{O}_6$ (or $\text{Li}_4\text{C}_6\text{O}_6$) in the electrolyte was 5 mg mL^{-1} . FT-IR spectra of the electrolyte without $\text{Li}_2\text{C}_6\text{O}_6$ (or $\text{Li}_4\text{C}_6\text{O}_6$), as-synthesized $\text{Li}_2\text{C}_6\text{O}_6$, and $\text{Li}_4\text{C}_6\text{O}_6$ powder were used as reference materials.

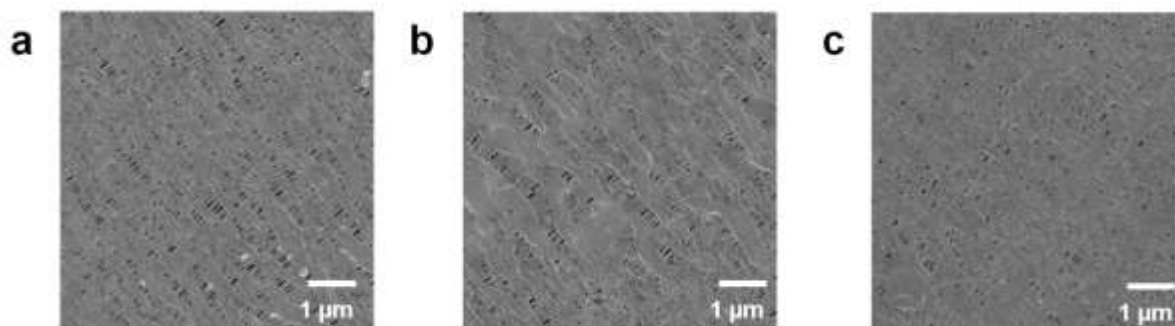


Figure S6. SEM micrographs of the separators are shown **a.** before cycling, **b.** after 5 cycles from 2.2 to 3.5 V, corresponding to the electrochemical reaction from $\text{Li}_2\text{C}_6\text{O}_6$ to $\text{Li}_4\text{C}_6\text{O}_6$, and **c.** after 5 cycles from 1.5 to 2.4 V, corresponding to the electrochemical reaction from $\text{Li}_4\text{C}_6\text{O}_6$ to $\text{Li}_6\text{C}_6\text{O}_6$.



Figure S7. Photo image of Fresh electrolyte and the electrolyte storing Li₂C₆O₆ and Li₄C₆O₆ for 48 hours (from left to right).

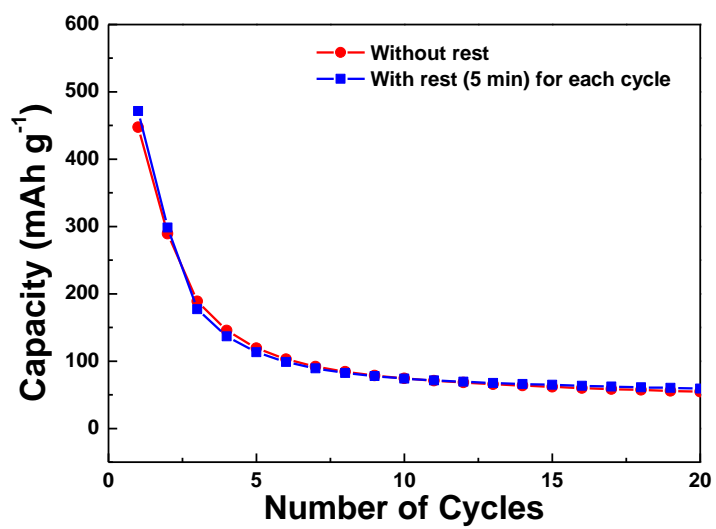


Figure S8. Cycle stability of $\text{Li}_2\text{C}_6\text{O}_6$. (red: battery cycling without rest time, blue: battery cycling with rest (5 min.) for each cycle).

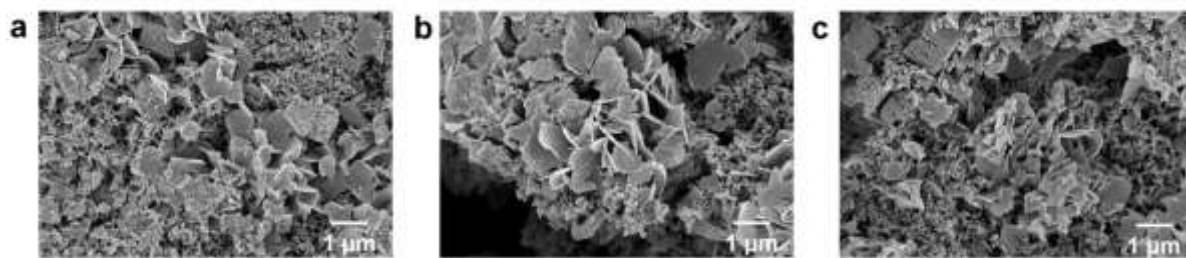


Figure S9. SEM micrographs of various regions of $\text{Li}_2\text{C}_6\text{O}_6$ electrodes after battery cycling show evidence of particle exfoliation over the entire electrode.

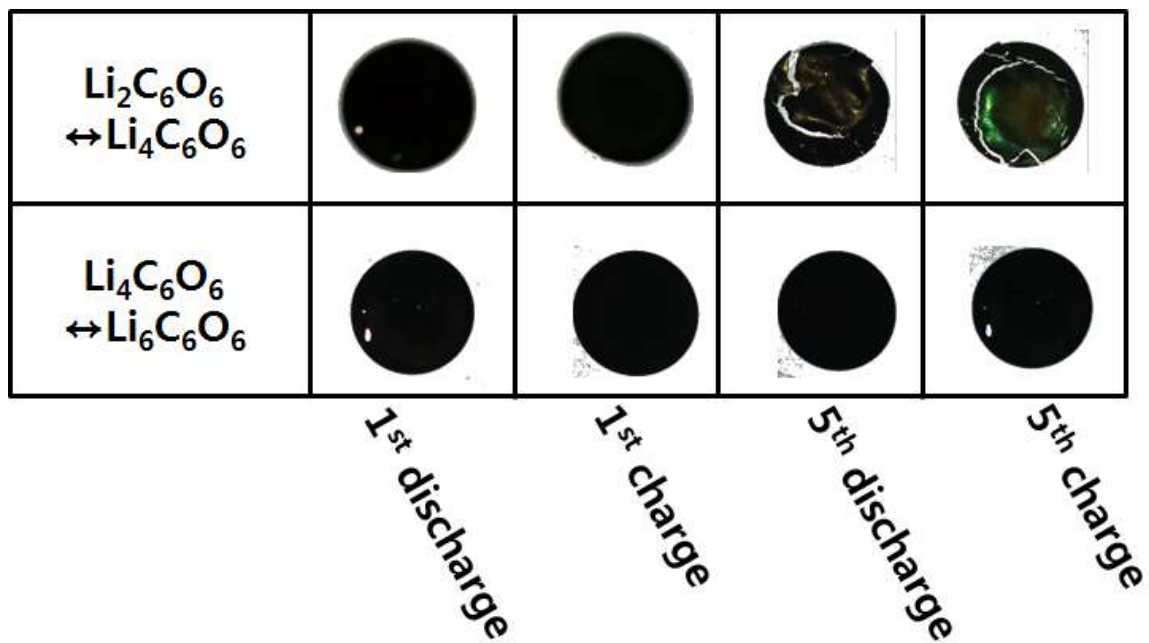


Figure S10. Photographs of the electrodes after battery cycling. While noticeable changes were not observed when $\text{Li}_4\text{C}_6\text{O}_6$ was repeatedly converted to $\text{Li}_6\text{C}_6\text{O}_6$, cracks were evident after $\text{Li}_2\text{C}_6\text{O}_6$ was repeatedly converted to $\text{Li}_4\text{C}_6\text{O}_6$.

References

- (1) Chen, H.; Armand, M.; Demailly, G.; Dolhem, F.; Poizot, P.; Tarascon, J.-M. From Biomass to a Renewable $\text{Li}_x\text{C}_6\text{O}_6$ Organic Electrode for Sustainable Li-Ion Batteries. *ChemSusChem* **2008**, *1*, 348-355.
- (2) Perdew, J. P.; Burke, K.; Ernzerhof, M. Generalized Gradient Approximation Made Simple. *Phys. Rev. Lett.* **1996**, *77*, 3865-3868.
- (3) Kresse, G.; Furthmüller, J. Efficiency of Ab-Initio Total Energy Calculations for Metals and Semiconductors Using a Plane-Wave Basis Set. *Comp. Mater. Sci.* **1996**, *6*, 15-50.
- (4) Kim, H.; Choi, J.-M.; Goddard, W. A. Universal Correction of Density Functional Theory to Include London Dispersion (up to Lr, Element 103). *J. Phys. Chem. Lett.* **2012**, *3*, 360-363.